On the Improvement of the Performance of the Optically Controlled Microwave Switch

D. A. M. Khalil and A. M. E. Safwat, *Student Member, IEEE*

***Abstract*— In this paper, a new design for the gap used as an optically controlled microwave switch is proposed. This new design is based on the use of a rib structure in the gap region. The proposed structure is studied using the finite-difference method (FDM). Obtained results show that for small gaplengths, the structure figure of merit, defined as the product of the ON/OFF ratio and the bandwidth, can be improved by about 38 dB $*$ GHz.**

***Index Terms*—Gap, optically controlled, rib structure.**

I. Introduction

AN OPTICALLY excited gap in a semiconductor microstrip transmission line, as shown in Fig. 1, has widespread use in high-speed photoconductive detectors [1]–[3] and optically controlled microwave devices [4]. The performance of this switch depends on its geometrical structure as well as substrate parameters [5]. This switch was first proposed by Auston in 1975 [6]. The switching action is produced by the incident optical beam. In the ON state, light of suitable wavelength is incident in the gap and the power is transmitted to the load through the created photoresistor. In the OFF state, the high-resistivity substrate reflect all the input signal, and the output port is isolated. The ratio between the transmitted power in both states is usually termed as ON/OFF ratio. To increase this value, we have to increase the value of the created photoconductance. This can be done by either increasing the incident optical power, which is not recommended, or reducing the dimensions of the gap, which in turn will reduce the operating bandwidth.

In this paper, the proposed new geometry for the gap enables an increase in the region of the interaction between the electric field and the created electron–hole pairs (EHP's), and thus, increases the value of the created photoconductance. As shown in Fig. 1, the region of the interaction between the electric field and the created EHP's is below the surface of the substrate in the gap, although a high electric field exists in the superstrate (air) over the gap. Thus, if we try to generate the EHP's not only below the air-substrate interface but also between or even above the gap, we may increase the created photoconductance. Fig. 2 shows the proposed geometry of the illuminated gap where it is filled by the semiconductor substrate. As will be seen later, this rib configuration does not significantly perturb the capacitance of the gap since the rib thickness is usually much smaller than the substrate height.

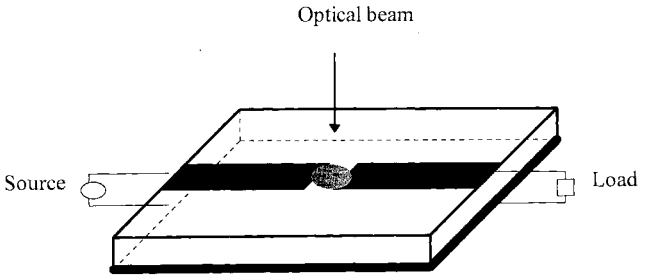

Fig. 1. Microwave switch—the optical beam controls the propagation of the microwave signal from the source to the load.

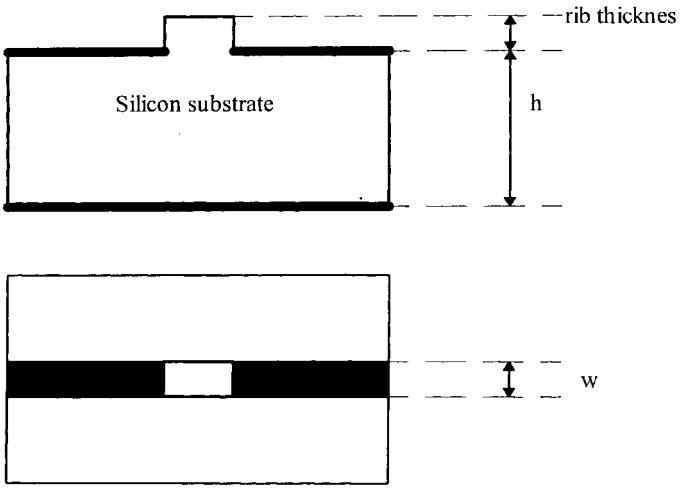

Fig. 2. Proposed structure to improve the performance of the optically controlled microwave switch.

In this paper, we will restrict ourselves to gaps with dimensions that are much smaller than the substrate height and the transmission-line width, since these gaps had shown good performances as optically controlled microwave switches [7], [8]. The analysis of the proposed structure is performed using the finite-difference method (FDM) and the optimization is based on a defined figure of merit for the switch.

II. Basic Theory

The lumped-element equivalent circuit of the illuminated gap is given in [5]. If we assume that: 1) gaplength is less than $h/10$ such that the gap can simply be represented in the dark

Manuscript received November 28, 1996; revised April 26, 1997.

D. A. M. Khalil is with Ain Shams University, Faculty of Engineering, Electronics and Communication Engineering Department, Abbasia, Cairo, Egypt.

A. M. E. Safwat was with Ain Shams University, Faculty of Engineering, Electronics and Communication Engineering Department, Abbasia, Cairo, Egypt. He is now with the Electrical Engineering Department, University of Maryland at College Park, College Park, MD 20742 USA.

Publisher Item Identifier S 0018-9480(97)05993-0.

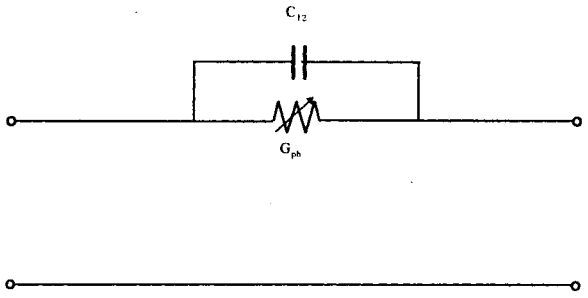

Fig. 3. The equivalent circuit of the illuminated gap after simplification.

state by a series capacitance [9]; 2) resistivity of the substrate in the dark state is very high; and 3) generated EHP's have no effect on the real part of the permittivity, then it has no effect on the capacitance. The same value of capacitance calculated in the dark state can be used to calculate S_{21} in the ON state. The simplified equivalent circuit for the illuminated gap is as shown in Fig. 3, where the photoconductance is assumed to be zero when the light is off. Knowing the capacitance and the photoconductance for each gaplength, S_{21} can be calculated using the following expression:

$$S_{21} = \frac{2Z_0G_{\rm ph} + j2Z_0\omega C_{12}}{1 + 2Z_0G_{\rm ph} + j2Z_0\omega C_{12}}. \tag{1}$$

S_{21} at dark is calculated using the same above expression but with $G_{\rm ph} = 0$. Thus, we can calculate the ON/OFF ratio given by S_{21} (ON) $-$ S_{21} (OFF) in decibels.

To evaluate the performance of this switch, it is required to determine the value of C_{12} and $G_{\rm ph}$. This needs to calculate the electric-field distribution and the carrier-concentration distribution in the gap. The field distribution is obtained using the FDM algorithm described in the following section.

III. The FD Algorithm

The FDM is now a well-known technique for the analysis of electrostatic problems. It has been applied to a wide range of two-dimensional (2-D) and three-dimensional (3-D) structures [10], [11].

Since we assume that the gaplength is much smaller than the stripwidth $(w/10)$, a 2-D mesh might be sufficient to determine the equivalent circuit of the gap. However, as the gaplength varies from 5 to 50 μm, we have chosen to use a nonuniform mesh as shown in Fig. 4. In this figure, the central point at (x_0, y_0) is in the middle of the gap and the separation h_i, h_j between the cells follows the rule of an arithmetic series.

To determine the electrostatic potential at every point in the mesh, we solve the Laplace-type equation

$$\nabla \cdot (\varepsilon \nabla V) = 0 \tag{2}$$

following the same procedure in [11] and using the boundary conditions given below.

1) In the substrate, far from the gap $(10h)$, we have a magnetic wall.
2) In the superstrate, the value of the potential at any point of the outer boundary in the superstrate is found by using the so-called asymptotic boundary conditions (ABC's) described in [12]. For geometries which mostly conform to rectangular boundaries, the absorbing operator $B1$, when expressed in Cartesian coordinates, takes the form given in [11].
3) The two electrodes on the surface have fixed potential difference of 1 V. The value of the voltage at the bottom is determined from the boundary condition of the electric field, which has only a normal component to the surface.

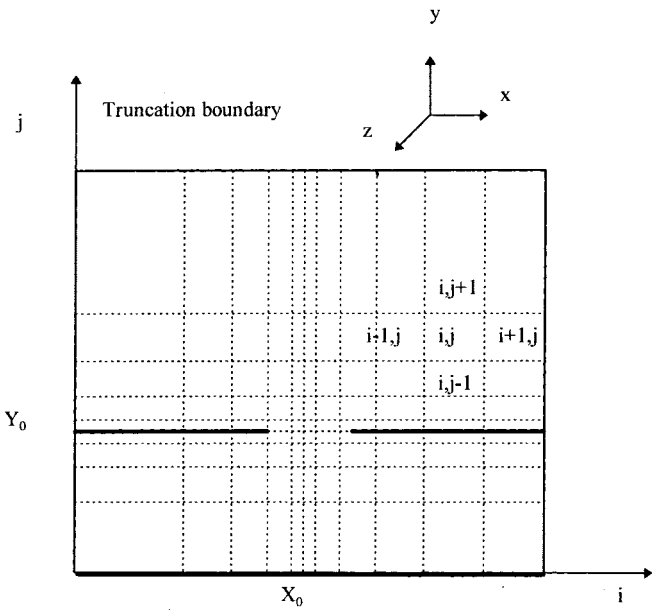

Fig. 4. Illustration of the numerical implementation of the FD solution.

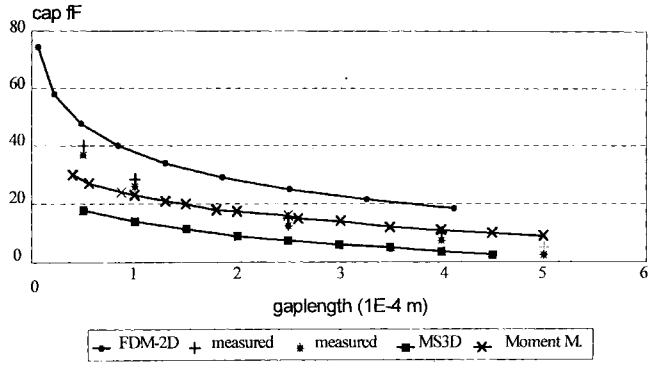

Fig. 5. The numerical results obtained compared to the moment method [13], the 3-D spectral-domain method [9], and measured values [13].

The capability of the algorithm to evaluate the capacitance of the gap in the microstrip transmission line is tested by considering a gap with the following dimensions $w = 508\ \mu$m, $h = 508\ \mu$m, and relative dielectric constant $= 8.875$. The mesh size is 300 $\times$ 200 points. The capacitance is calculated using

$$C = \frac{Q_{\rm tot}}{V_{\rm diff}} = \frac{-\varepsilon_0 \int_S \varepsilon_r(x,y) \nabla V \cdot n\, ds}{V_{\rm diff}} \tag{3}$$

where $Q_{\rm tot}$ is the total charge stored on the conductor enclosed by the surface placed at the plane yz, as shown in Fig. 4. Fig. 5 shows the numerical results obtained compared to the moment method [13], the 3-D spectral-domain method [9], and

measured values [13]. From these results, we can see that there is good agreement between the numerical results obtained and the asymptotic of the moment method and the measured data for small gaplengths ($L_g < h/10$ and $L_g < w/10$). The error at $L_g = 50$ μm is about 10% from the measured data. This error increases to a factor of 2 at $l_g = 400$ μm. For a large gap, a 3-D mesh is required as in [10]. This is expected since in 2-D analysis, we do not take into consideration either the distribution of the current on the strips or the fringing effect.

IV. Numerical Results

To study the performance of the optically controlled microwave switch, we need to calculate its equivalent circuit. Equation (3) is used to determine the value of the capacitance while the photoconductance is obtained using

$$G_{\rm ph} = \frac{I_{\rm tot}}{V_{\rm diff}} = \frac{-\int_S \sigma(x,y)\nabla V \cdot n\, ds}{V_{\rm diff}} \tag{4}$$

where the conductivity $\sigma(x,y)$ resulting from the incident light is given in [14]. Using the following parameters: $w = 410$ μm, $h = 500$ μm, $\varepsilon_r = 11.8$, spot diameter $= 410$ μm, incident optical power $= 300$ mW, $\mu_n = 0.0135$ m^2/V$\cdot$s, $\mu_p = 0.045$ m^2/V$\cdot$s, absorption coefficient $\alpha = 10^7$ m^{-1}, incident wavelength $\lambda = 0.4$ μm. These values correspond to a transmission line with characteristic impedance equal to 50 Ω on a silicon substrate. After the determination of the capacitance and the conductance for each gaplength, we calculate S_{21} using (1) in the ON and OFF states and then the ON/OFF ratio. Fig. 6 shows the variation of the capacitance with the rib thickness for different gaplengths. As predicted, the value of the capacitance slightly increases due to the small value of the rib thickness with regard to the substrate height. Fig. 7 shows the variation of the created photoconductance with the rib thickness. The relation obtained has a bell shape. This could be explained by the interaction between the electric field and the created EHP's. If the EHP's are in the region of a strong electric field, the photoconductance has a greater value, otherwise they are in the region of a weak electric field and the value of the created photoconductance is small. In Fig. 7, we can also see that the rib thickness required for maximum photoconductance is not the same for all gaplengths. This is because with a gap in a microstrip transmission line, the electric field has a maximum value near the gap surface [15] which reduces as we penetrate into the semiconductor. The rate of its decrease is higher for small gaplength and, as a consequence, the rib thickness required to get a maximum photoconductance increases as the gaplength increases.

The ON/OFF ratio is calculated for different gaplengths and rib thickness. A sample of these results is shown in Fig. 8. We can see that as we increase the rib thickness, the ON/OFF ratio first increases until it reaches a maximum value at a certain rib thickness and then it decreases. This is because the created EHP's go to the region of weak electric field. At the extreme, the electric field is zero and the created photoconductance has no effect on the performance of the optically controlled microwave switch. On the other hand, the bandwidth has not been reduced because the variation of the capacitance is negligible, as shown in Fig. 6. As predicted, the rib thickness required to get a maximum ON/OFF ratio increases as the gaplength increases.

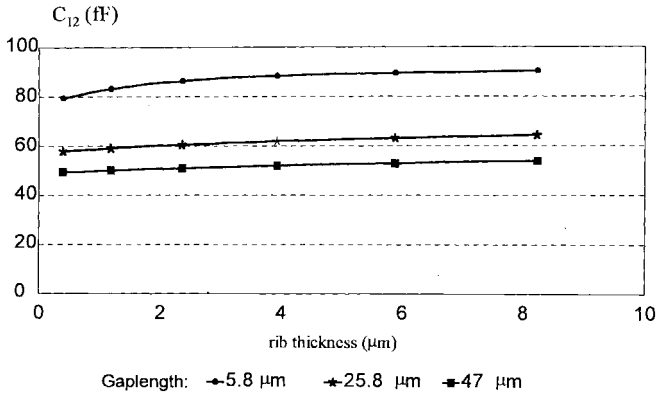

Fig. 6. The variation of the capacitance with the rib thickness for different gaplengths.

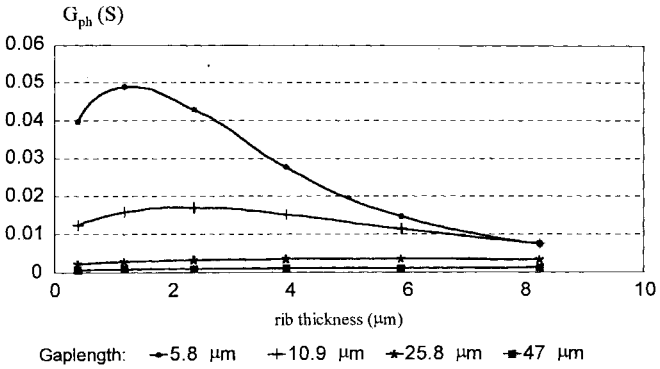

Fig. 7. The variation of the created photoconductance with the rib thickness for different gaplengths.

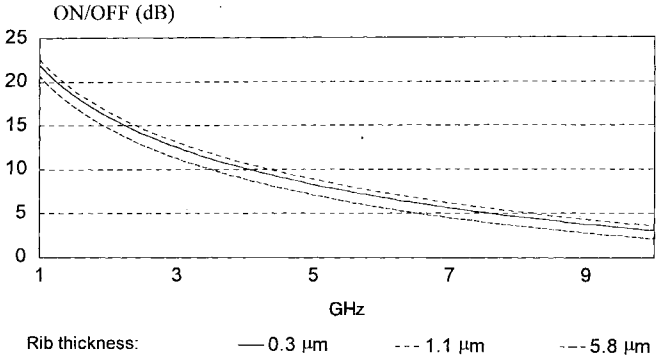

Fig. 8. The ON/OFF ratio for gaplength $= 10.9$ μm and different rib thickness.

To determine the optimum rib thickness for each gaplength, we define the figure of merit of the structure as follows:

$$\text{Figure of merit} = \text{Gain} * \text{operating Bandwidth} \tag{5}$$

where the operating bandwidth is the frequency at which the ON/OFF ratio equals $= 5$ dB. This figure of merit normalized with regard to the case of no rib is plotted in Fig. 9 as a function of the rib thickness where the gaplength is used as a parameter. For small gaplengths, the ON/OFF ratio is initially

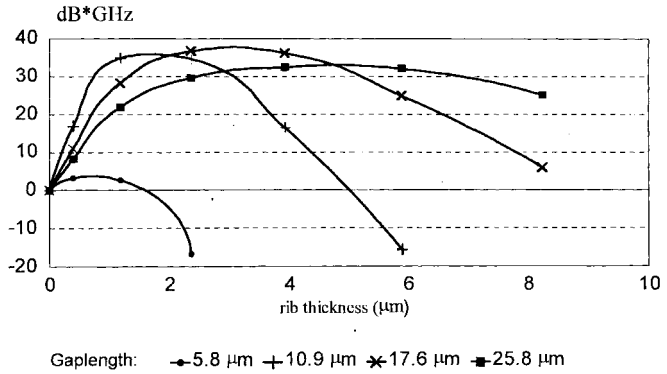

Fig. 9. The normalized figure of merit as a function of the rib thickness for different gaplengths.

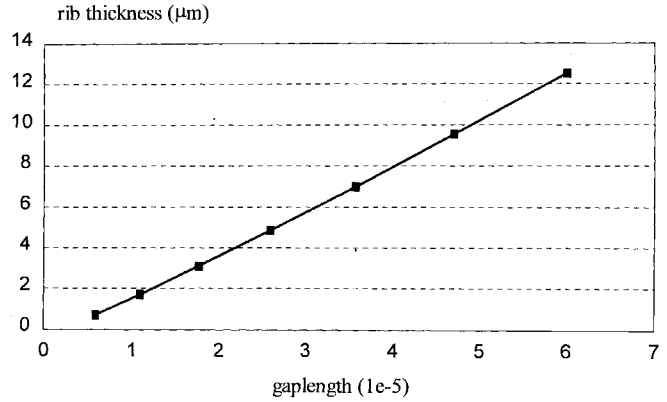

Fig. 10. The optimum rib thickness for each gaplength.

high and the presence of the rib increases this ratio but with a small value. If we increase the gaplength, the ON/OFF ratio is initially small and in the presence of the rib it tends to increase. An increase in the figure of merit by about 37 dB $*$ GHz is obtained at $L_g = 17.6\ \mu$m while only 5–8 dB $*$ GHz is obtained at $L_g = 60\ \mu$m. From Fig. 9, we can approximately determine the optimum rib thickness for each gaplength. This is shown in Fig. 10. This relation tends to be linear, i.e., the rib thickness increases as the gaplength increases. This can be explained by the relation between the electric field and the gaplength. As the gaplength increases, the electric field is reduced and broadened in the direction normal to the gap. This makes the optimum rib thickness required increase such that the region of the interaction between the electric field and the created EHP's increases. The effect of varying the absorption coefficient is also studied. The optimum rib thickness is found to be nearly independent on α, i.e., the factor that prevails in determining the optimum rib thickness is the distribution of the electric field.

V. Conclusion

In this paper, we have studied the optically controlled microwave switch. This study is based on a simplified equivalent circuit for the gap in the dark and illuminated states. The elements of the gap equivalent circuit have been calculated using the FDM with nonuniform mesh and absorbing-boundary conditions. To enhance the performance of the switch, a rib structure is proposed for the gap connecting the two microstrip lines. The performance analysis of such a rib-structured switch shows that an optimum rib thickness exists. This optimum rib thickness is linearly proportional to the gaplength. At this thickness, the switch figure of merit (defined as the product of the ON/OFF ratio and the bandwidth) is maximum. An increase in the figure of merit in the order of 40 dB $\cdot$ GHz at small gaplengths or 5–8 dB $\cdot$ GHz at large gaplengths have been predicted. Such optimization is of great interest as it enables the reduction of the optical power required for switching, which is one of the major factors limiting the use of such devices today.

References

[1] D. H. Auston *et al.*, "An amorphous silicon photodetector for picosecond pulses," *Appl. Phys. Lett.*, vol. 36, no. 1, pp. 66–68, Jan. 1980.
[2] ——, "Picosecond optoelectronic detection, sampling, and correlation measurements in amorphous semiconductors," *Appl. Phys. Lett.*, vol. 37, no. 4, pp. 371–372, Aug. 1980.
[3] S. Huang *et al.*, "On-wafer photoconductive sampling of MMIC's," *IEEE Trans. Microwave Theory Tech.*, vol. 40, pp. 2312–2320, Dec. 1992.
[4] I. Anderson and S. T. Eng, "Phase and amplitude characteristics of InP:Fe modified interdigitated gap photoconductive microwave switches," *IEEE Trans. Microwave Theory Tech.*, vol. 37, pp. 729–733, Apr. 1989.
[5] S. Gevorgian, "Design considerations for an optically excited semiconductor microstrip gap at microwave frequencies," *Proc. Inst. Elect. Eng.*, vol. 139, pt. J, pp. 153–157, Apr. 1992.
[6] A. M. Johnson and D. H. Auston, "Microwave switching by picosecond photoconductivity," *IEEE, J. Quantum Electron.*, vol. QE-11, pp. 283–287, June 1975.
[7] S. Sani, E. Pic, S. Tedjini, and M. Bouthinon, "Photocommutateur sur GaAs:Cr^+ a large bande en technologie guide d'onde coplanaire," Journées Optiques et microondes, Chapitre français, presented at the *IEEE-MTT Symp. Conf.*, Nov. 26–27, 1992.
[8] S. Sani, "Photo-commutateur a large bande en technologies guide d'ondes coplanaire et microruban realize sur GaAs:Cr^+ et sur Si," Ph.D. dissertation, LEMO, IMPG, Grenoble, France, 1992.
[9] A. Vilcot, "Contribution a la modelization en micro-ondes des lignes et discontinuites planaires," Ph.D. dissertation, LEMO, IMPG, Grenoble, France, 1992.
[10] M. Naghed and I. Wolff, "Equivalent capacitances of coplanar waveguide discontinuities and interdigitated capacitors using a three dimensional finite difference method," *IEEE Trans. Microwave Theory Tech.*, vol. 38, pp. 1808–1815, Dec. 1990.
[11] B. Beker and G. Cokkinides, "Computer-aided quasistatic analysis of coplanar transmission lines for microwave integrated circuits using the finite difference method," *Int. J. Microwave and Millimeter-Wave Comput.-Aided Eng.*, vol. 4, no. 1, pp. 111–118, 1994.
[12] A. Khebir, A. Kouki, and R. Mittra, "Higher order asymptotic boundary condition for the finite element modeling of two dimensional transmission line structures," *IEEE Trans. Microwave Theory Tech.*, vol. 38, pp. 1433–1438, Oct. 1990.
[13] H. Yang, N. Alexopoulos, and D. Jackson, "Microstrip open-end and gap discontinuities in a substrate and superstrate structure," *IEEE Trans. Microwave Theory Tech.*, vol. 37, pp. 1542–1546, Oct. 1989.
[14] W. Platte and B. Sauerer, "Optically CW-induced losses in semiconductor coplanar waveguides," *IEEE Trans. Microwave Theory Tech.*, vol. 37, pp. 139–148, Jan. 1989.
[15] D. Marcuse, "Optimal electrode design for integrated optics modulators," *IEEE J. Quantum Electron.*, vol. QE-18, pp. 393–398, Mar. 1982.

D. A. M. Khalil, for a biography, see this issue, p. 1357.

A. M. E. Safwat, (S'91), for photograph and biography, see this issue, p. 1357.